

---

# Phase Morphology and Mechanical Properties of Aliphatic Waterborne Polyurethane-ureas: Effect of 1,6-hexamethylene Diisocyanate (HDI)/Isophorone Diisocyanate (IPDI) Ratio

Heqing Fu, Kang Liu, Caibin Yan, Weifeng Chen, and Yin Wang

School of Chemistry and Chemical Engineering, South China University of Technology, Guangdong, Guangzhou 510640, China

Received: 10 September 2013, Accepted: 13 October 2014

## SUMMARY

Aliphatic waterborne polyurethane-ureas (WPUU) were prepared using 1,6-hexamethylene diisocyanate (HDI) and isophorone diisocyanate (IPDI) as mixed diisocyanates. The effects of the HDI/IPDI ratio on the phase morphology of WPUU films including the hydrogen bonding, crystallization of the soft segment and hard segment, and phase separation were investigated. The relationship between the phase morphology and the mechanical properties was also studied. The FTIR spectrum showed that the hydrogen bonding degree in the hard segments increased as the HDI/IPDI ratio increased. XRD analysis revealed the excellent crystallinity of WPUU films. DSC analysis indicated that the degree of phase separation was improved with increasing HDI/IPDI ratio, and DMA analysis showed that the storage modulus of the WPUU film increased at first and then decreased. When the HDI/IPDI ratio was 4:1, the WPUU films exhibited high tensile strength.

**Keywords:** Waterborne polyurethane-ureas, Phase morphology, Mechanical Properties, HDI/IPDI ratio

---

## 1. INTRODUCTION

Polyurethane (PU) is one kind of linear-[A-B]<sub>n</sub>-block copolymer. One of the blocks is relatively flexible with a low solubility parameter and is referred to as the soft segment, while the other block is either highly polar and/or stiff with a high solubility parameter and is known as the hard segment<sup>1</sup>. The soft segment contains polyester diol or polyether diol, while the hard segment is derived from diisocyanate, such as isophorone diisocyanate (IPDI), 1,6-hexamethylene diisocyanate (HDI), 4,4'-diphenylmethane diisocyanate (MDI), and short chain extender like 1,4-butanediol, or ethylene diamine<sup>2, 3</sup>. The chain of polyurethane is built up from more or less immiscible segments, which can segregate above the glass transition

temperature of the soft phase. This process is called phase separation<sup>4</sup>. The extent of phase separation and the composition of the phases decisively influence the final properties of the material. The unique properties of polyurethane are related to the phase separation, in which the hard segments act as thermally-reversible physical crosslinking sites within the soft matrix, resulting in excellent thermoplastic and mechanical properties for the polyurethanes<sup>5,6</sup>. There are many factors affecting this morphology: hydrogen bonding interaction between internal /external segments, the degree of crystallization of the hard or soft segment, segmental polarity difference, segmental length, overall composition and molecular weight. The morphology of these microdomains strongly affects the

mechanical properties of polyurethanes. Therefore, it is important to understand the relationships between the phase morphology and mechanical properties of polyurethane film. Some articles have studied the phase morphology of polyurethane and its effect on properties<sup>11-15</sup>. Mishra *et al.*<sup>11</sup> studied the effect of chain structure on the morphology of polyurethane at various length scale. Two-phase morphology was seen in aliphatic polyurethanes, and mostly single phase was observed in aromatic polyurethanes. AFM topographs exhibited banded domains for aliphatic PUs and the dimensions of the domains gradually decreased with increasing hard segment content. Sheth *et al.*<sup>12</sup> reported a hard segment phase connectivity and percolation model for segmented poly(urethane urea) copolymers. The results showed that the tapping-mode AFM phase image of the poly(urethane urea) sample without hard segment branching exhibited the form of long ribbon-like hard domains percolating in the soft matrix.

---

Correspondence to: Heqing Fu (fuhq@scut.edu.cn), Tel: 086-020-87114919, Fax: 086-020-87112047

©Smithers Information Ltd., 2015

Culin *et al.*<sup>13</sup> studied the effect of functional group concentration on the phase morphology of functionalized polyester polyurethanes. They found that the changes of crystallinity and morphology were due to the incorporation of carboxylic functional groups in the hard segment. The phase separation, the degree of crystallinity and the size of spherulites depended on the interactions imposed by functional groups. A critical concentration of functional groups was observed at which the crystallizability reached its maximum. The principal diisocyanate raw materials for synthesis of polyurethane include TDI, MDI, HDI, IPDI etc.<sup>16-17</sup>. Due to the presence of the rigid aromatic ring, the aromatic-based polyurethanes exhibit high strength and high modulus; however, the colour of the film is easy to turn yellow, which limits the wide use of aromatic diisocyanates<sup>18</sup>. However, polyurethane derived from aliphatic diisocyanates provides outstanding oxidation resistance, light stability, resistance to hydrolysis and thermal degradation<sup>19</sup>. Therefore, aliphatic diisocyanates are often used in polyurethane.

In this study, aliphatic diisocyanates HDI and IPDI were used as mixed diisocyanates to synthesize waterborne polyurethane-ureas. The effects of the HDI/IPDI ratio on the phase morphology of WPUU films including the hydrogen bonding, crystallization of the soft and hard segments, and phase separation, was studied by FT-IR, XRD, DSC and AFM. The viscoelastic behaviour of WPUU films was characterized using DMA.

The relationship between the phase morphology and the mechanical properties was also investigated.

Although there were some previous reports about the phase morphology in polyurethane and its effect on properties, there was no report about the HDI/IPDI ratio on the morphology and mechanical properties of aliphatic waterborne polyurethane-ureas synthesized from mixed diisocyanates.

## 2. EXPERIMENTAL SECTION

### 2.1 Materials

1,6-hexamethylene diisocyanate (HDI) and isophorone diisocyanate (IPDI) (supplied by Bayer Co., Germany), 1,4-butylene adipate glycol (PBA,  $M_n=2000$ ) (supplied by Donghao Resin Co. Ltd., China), dimethylol propionic acid (DMPA) (supplied by Perstop, Sweden), 1,4-butanediol (BDO) (supplied by Jiangmen Carpoly Chemical Co. Ltd., China), N-methyl pyrrolidone (NMP) (supplied by Shanghai Chemical Agent Factory, China), triethylamine (TEA) and ethylene diamine (EDA) (supplied by Shanghai Fine Chemical Agent Factory, China), dibutyltin dilaurate (DBTDL) (supplied by Shanghai Lingfeng Chemical Agent Co. Ltd, China), acetone (supplied by Guangzhou Fine Chemical Factory, China).

### 2.2 Synthesis of Waterborne Polyurethane-Ureas (WPUU)

The waterborne polyurethane-ureas were prepared through prepolymer

process. A dry 1000 mL four-necked flask equipped with a mechanical stirrer, thermometer, condenser and a nitrogen inlet was placed in a constant temperature water bath. Stoichiometric proportions of HDI, IPDI, PBA and the catalyst DBTDL were added into the reactor under nitrogen atmosphere. The reaction was carried out at 80 °C for about 2.5 h to obtain an NCO-terminated prepolymer. After that, DMPA and BDO dissolved in NMP were added into the flask while the temperature was at 75 °C, and the reaction proceeded until the residual NCO content reached the desired value (determined by the di-n-dibutylamine titration). The prepolymer was cooled to 40 °C and the carboxylic acid in the prepolymer was neutralized by TEA aqueous solution for 30 min to obtain the ionomer (before the neutralization, a little acetone was added to decrease the viscosity of the prepolymer). Then the ionomer was dispersed in a stoichiometric amount of deionized water with vigorous stirring followed by EDA chain extender. The stable waterborne polyurethane-ureas were finally obtained after removing the acetone by vacuum distillation. The formulations are presented in **Table 1**.

### 2.3 Preparation of WPUU Films

The WPUU films were prepared by casting the dispersion on a PTFE mould and allowing the films to dry at room temperature for 7 days. Afterwards the films were placed in an oven in vacuum at 60 °C for 4 hours. Then they were used for characterization.

**Table 1. Formulation of the waterborne polyurethane-ureas**

Sample	PBA (mol)	HDI/IPDI	DMPA (mol)	1,4-BD (mol)	EDA (mol)	TEA (mol)	Hard segment (wt.%)
WPUU-1	0.184	1:1	0.092	0.196	0.004	0.092	33
WPUU-2	0.180	2:1	0.092	0.200	0.004	0.092	
WPUU-3	0.176	3:1	0.092	0.204	0.004	0.092	
WPUU-4	0.172	4:1	0.092	0.208	0.004	0.092	
WPUU-5	0.172	5:1	0.092	0.208	0.004	0.092	

Note: NCO/OH = 1.7, wt(DMPA) = 2.5 % and solid content = 40 %

## 2.4 Instrumental Characterization

The FT-IR spectra of the polyurethane-ureas were characterized by a Perkin-Elmer Spectrum 2000 infrared spectrophotometer in the range 400 ~ 4000  $\text{cm}^{-1}$  at 25 °C. X-ray diffraction (XRD) was performed on a D8 Advance apparatus (Bruker, Germany) in the range of  $2\theta=10\sim70^\circ$ , with a nickel-filtered Cu K-radiation at an operation voltage of 40 kV. Differential scanning calorimetry (DSC) was measured by a TA Instruments Q20 DSC analyzer from -80 °C to 250 °C at a heating rate of 10 °C/min under nitrogen atmosphere. Atomic force microscopy (AFM) was performed using a instrument (CSPM 2003) with 27  $\mu\text{m}\times 27\ \mu\text{m}$  scanned area and images were acquired under ambient conditions in contact mode using a nanoprobe cantilever. Dynamic mechanical thermal analysis (DMA) was performed on a DMA 242C (Netzsch, Germany) in tension mode, from -100 °C to 150 °C at 1 Hz, with a heating rate of 5 °C/min. The tensile properties of the films were measured at room temperature on an Instron tension meter Model 3367. A crosshead rate of 100 mm/min was used to determine the ultimate tensile strength and the elongation at break.

## 3. RESULTS AND DISCUSSION

### 3.1 FTIR Analysis

The segmental structure in WPUU can be related to the interactions of hydrogen bonding in the intra/inter segments. FTIR spectroscopy was used to determine the effect of HDI/IPDI ratio on the interactions of hydrogen bonding in the system. As seen from **Figure 1**, no peaks were observed at 2270  $\text{cm}^{-1}$  in the spectra. This is because the complete reaction of NCO groups in the dispersion procedure<sup>20</sup>. Meanwhile, the peaks corresponding to the N-H stretching mode at 3365  $\text{cm}^{-1}$ , the carbonyl stretching absorption peak at 1730  $\text{cm}^{-1}$ , and the N-H bending vibration at 1550  $\text{cm}^{-1}$  were

observed in the FTIR spectra which provided evidence for the formation of a urethane.

It was reported that the infrared absorption corresponding to the hydrogen bonded N-H and C=O groups could slightly shift to a lower frequency than that of free N-H and C=O groups<sup>21</sup>.

Meanwhile, the C=O absorption peaks of urethane groups were affected by the C=O absorption peaks of the polyester in the WPUU<sup>22</sup>. The vibration of the C=O in the urea linkages was therefore selected to investigate the formation of hydrogen bonding. The FTIR spectra of different WPUU films in the C=O stretch region are shown in **Figure 2**.

**Figure 1.** FTIR spectra of WPUU films with different HDI/IPDI mole ratio

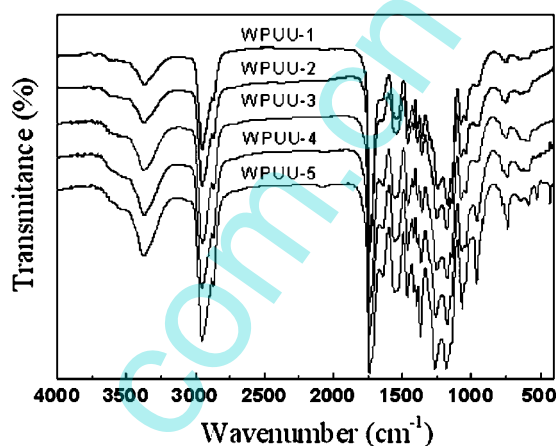
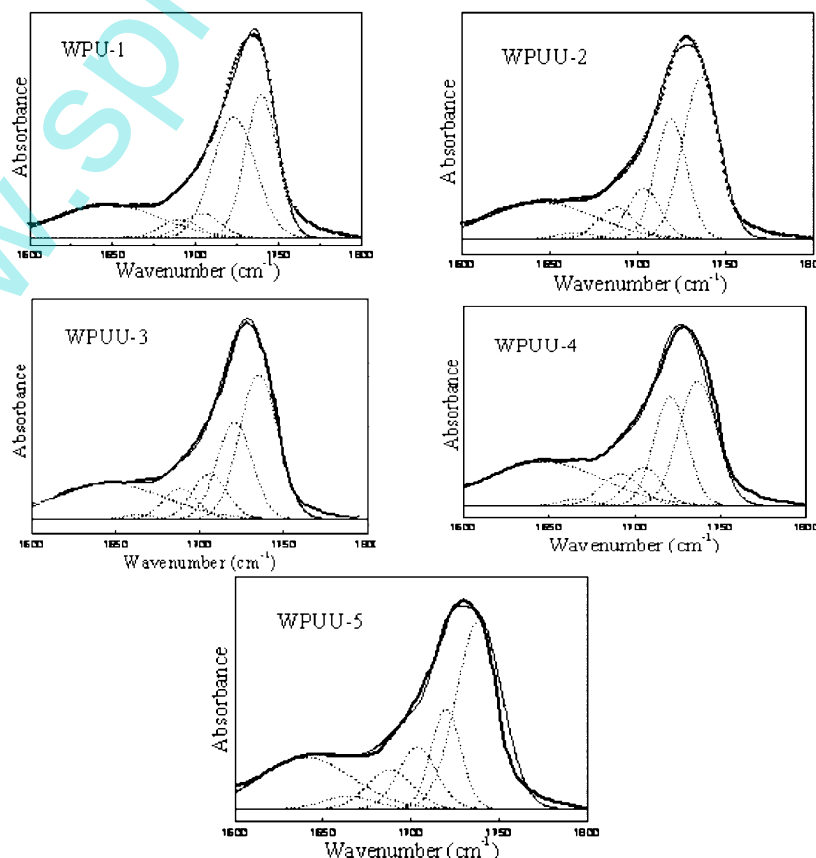


**Figure 2.** FTIR spectra and curve fittings in the carbonyl region for WPUUs (solid line: original result; dashed line: curved-fitting result)



The Gaussian curve method was used to analyze the C=O absorption region by using Origin<sup>®</sup> software. The results are presented in **Tables 2** and **3**. The hydrogen bonding index R is used to indicate the degree of hydrogen bonding in the urea groups, defined as the quotient of the absorption area ratio between H-bonded C=O and free C=O. A larger value of R indicates that more H-bonded C=O groups exist in the urea moieties. The degrees of ordered and disordered H-bonded C=O in the H-bonded ureas are defined as follows:

$$R = \frac{\text{Area}(\text{bonded}, \text{UA})}{\text{Area}(\text{free}, \text{UA})} \quad (1)$$

$$X_{d, \text{UA}} = \frac{\text{Area}(d, \text{UA})}{\text{Area}(\text{bonded}, \text{UA})} = \frac{\text{Area}(d, \text{UA})}{\text{Area}(d, \text{UA}) + \text{Area}(o, \text{UA})} \quad (2)$$

$$X_{o, \text{UA}} = \frac{\text{Area}(o, \text{UA})}{\text{Area}(\text{bonded}, \text{UA})} = \frac{\text{Area}(o, \text{UA})}{\text{Area}(d, \text{UA}) + \text{Area}(o, \text{UA})} \quad (3)$$

As shown in **Table 3**, with the increasing of HDI/IPDI ratio, the R,  $X_{o, \text{UA}}$  increased, up to 77.97 % and 90.84% respectively, while  $X_{d, \text{UA}}$  decreased from 75.38% to 9.16%. This indicated that the degree of hydrogen bonding in the hard segments increased and the regularity of segmental structure was improved. On the one hand, the ordered linear chemical structure of HDI leads to more ordered arrangement of hard segments and enhance the hydrogen bonding interaction between hard segments because of its chain mobility. On the other hand, the highly hydrogen-bonded hard segments act as physical crosslinks and increase hydrogen bonding interaction within hard segments, restricting segmental motion of the polymer chain, which results in more significant phase separation between hard and soft segments. This would promote the formation of ordered hydrogen-bonded structure in the hard segments. Hence, the degree of hydrogen bonding and its regularity in the hard segments was enhanced as the HDI/IPDI ratio increased.

**Table 2.** Assignment of the absorption bands in the carbonyl region of the FTIR spectra for WPUU

Wavenumber (cm <sup>-1</sup> )	Assignment
1750-1730	Free C=O of urethane linkages and polyester
1730-1715	Disordered H-bonded C=O of urethane linkages and H-bonded C=O of polyester
1710-1700	Ordered H-bonded C=O of urethane linkages
1690-1680	Free C=O of urea linkages
1680-1650	Disordered H-bonded C=O of urea linkages
1650-1630	Order H-bonded C=O of urea linkages

**Table 3.** Curve fitting results of urea carbonyl region for WPUUs

Sample	Peak area (%)			R
	$X_{b, \text{UA}}$ (%)	$X_{d, \text{UA}}$ (%)	$X_{o, \text{UA}}$ (%)	
WPUU-1	60.89	75.38	24.62	1.57
WPUU-2	64.67	50.09	49.91	1.83
WPUU-3	73.88	33.07	66.93	2.82
WPUU-4	75.19	18.78	81.22	3.03
WPUU-5	77.97	9.16	90.84	3.54

### 3.2 XRD Analysis

WPUU exhibits a high degree of crystallinity due to the hydrogen bonding and the ordered segmental structure in the system. Therefore, XRD analysis was used to examine the crystallinity of WPUU, and the results are shown in **Figure 3**. As can be seen, the polyol PBA exhibited excellent crystallinity and showed three significant sharp diffraction peaks at  $2\theta$  values of 21.5°, 22.5° and 24°. The WPUU based on this kind of polyol presented identical diffraction peaks at 21.5°, 22.5° and 24°, and exhibited an extra sharp diffraction peak at about 49°, which might be attributed to the crystallization of hard segments. This implied that both the soft segment and the hard segment had good crystallinity. With decreasing HDI/IPDI ratio, the intensity of the diffraction peaks at 21.5°, 22.5°, 24° and 49° decreased, which demonstrated that the asymmetrical IPDI destroyed the structural regularity of the soft and hard segments. On the one side, the hard segments were unable to pack compactly with the IPDI, leading to the decay of the hydrogen-bonding ability of the hard segments, as discussed in section 3.1. As a result, the symmetry and regularity of the hard domains were disrupted and their crystallinity decreased<sup>23</sup>. On the other hand, due to the lack of compact packing of the hard segments, some of them dissolved in the soft matrix, which enhanced the interaction between the soft and hard segments and generated a higher degree of phase mixing (will be analyzed by DSC later). Therefore, the crystallinity of the soft and hard segments decreased with decreasing HDI/IPDI ratio.

### 3.3 DSC Analysis

The effect of the HDI/IPDI ratio on the phase separation of WPUU was studied by DSC, as illustrated in **Figure 4**. The glass transition temperature ( $T_{\text{gss}}$ ) of the soft segments in WPUU is at -50 °C. Two melting endothermic peaks were observed in DSC curves from 45 °C to 55 °C ( $T_{\text{m1}}$ ) and 210 °C to 225 °C

( $T_{m2}$ ), corresponding to the crystalline melting endothermic peaks of soft and hard segments respectively<sup>24</sup>. With increasing HDI/IPDI ratio,  $T_{gss}$  shifted to lower temperature, from -49.9 °C to -53.4 °C, and the  $T_{m2}$  associated with the crystalline hard segments shifted to a higher one. This implies that the thermodynamic incompatibility between soft and hard segment was improved, and a higher phase-separation was generated<sup>25</sup>. This contributes to decreasing of the interaction between soft and hard segments. However, the value of  $T_{m1}$  associated with the crystalline soft segments varies irregularly.

There were two significant melting endothermic peaks observed in the DSC curves, and the enthalpies of fusion related to the melting peaks presented in **Table 4**. From the results it was found that the  $\Delta H_1$  and  $\Delta H_2$  increased with the increasing of HDI/IPDI ratio, which indicated that the crystallinities of the soft and hard segments were improved. On the one hand, due to the formation of ordered hydrogen bonding and more compact packing of hard segments, the hard segments exhibited improved crystallinity. On the other hand, because of the increased phase separation between soft and hard segments, the soft segments presented the excellent crystallinity of a polyester<sup>26</sup>. This result is consistent with that of XRD as discussed previously.

### 3.4 AFM Analysis

The phase morphology of WPUU was investigated by AFM, as shown in

Figure 3. XRD spectra of WPUU with different HDI/IPDI ratio

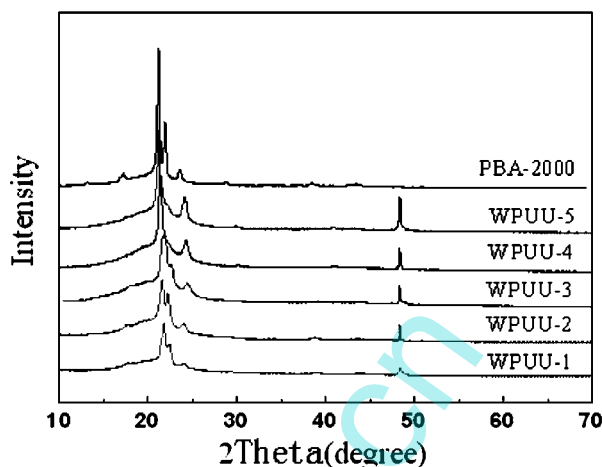
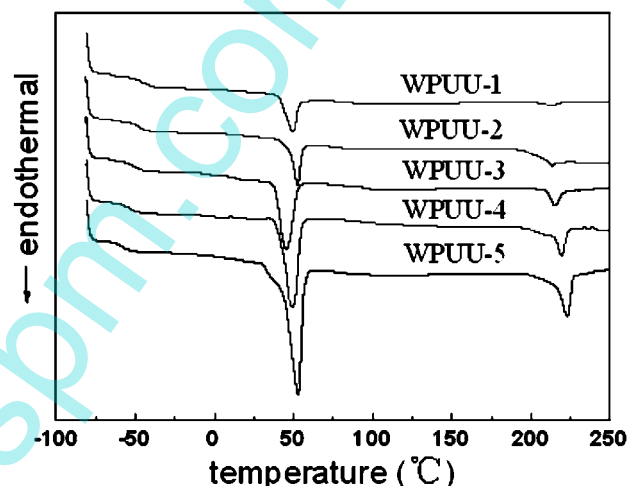


Figure 4. DSC thermograms of WPUU films with different HDI/IPDI ratio



**Figures 5 and 6.** A bunch of sharply outlined shapes can be observed in **Figure 6**, which correspond to the bright crest in **Figure 5**, assigned to the hard phase because of its high surface energy<sup>27</sup>. The dark trough distributed in the Figure are related to the soft phase.

The WPUU-1 show a disordered phase morphology with the bright crests dispersed irregularly in the continuous soft matrix, whereas the WPUU-5 presents a ordered arrangement of the bright crests, with an increased average distance between the hard segments (more obvious in the three-dimensional

Table 4. DSC scan results for the WPUU with different HDI/IPDI ratio

Sample	$T_{gss}^a$ (°C)	$T_{gss}^b$ (°C)	$T_{m1}$ (°C)	$\Delta H_1$ (J/g)	$T_{m2}$ (°C)	$\Delta H_2$ (J/g)
WPUU-1	-39.5	-54.2	49.0	11.57	213.4	1.01
WPUU-2	-40.8	-55.6	50.1	13.76	214.0	3.94
WPUU-3	-41.6	-56.8	48.8	26.57	215.5	5.44
WPUU-4	-42.2	-57.2	49.2	29.94	219.3	6.96
WPUU-5	-42.6	-60.1	52.4	36.46	224.6	12.04

a: the value of  $T_{gss}$  was obtained by DMA b: the value of  $T_{gss}$  was obtained by DSC

images). This result verified directly that the extent of phase separation of WPUU increased with increased HDI/IPDI ratio.

### 3.5 Dynamic Mechanical Analysis

The viscoelastic properties of the WPUU films were characterized by the dynamic mechanical analysis, and the variations of the storage modulus ( $E'$ ) and loss factor ( $\tan \delta$ ) are shown in **Figures 7** and **8**, respectively.  $E'$  is a measurement of the mechanical energy stored under loading<sup>28</sup>. The value of  $\tan \delta$  can be defined as the quotient of loss modulus ( $E''$ ) and storage modulus, i.e.  $\tan \delta = E''/E'$ <sup>29</sup>. The peak of  $\tan \delta$  corresponds to the glass transition temperature ( $T_{gss}$ ) of the soft segments, and it also correspond to the phase-separation degree. However, the value of  $T_{gss}$  obtained from DMA is slightly higher than that from DSC, which is in agreement with the expectations.

In **Figure 7**, it can be observed that the storage modulus increased first and then decreased, and the storage modulus of WPUU film is largest when the HDI/IPDI ratio is 4:1. This may be the effect of hydrogen bonding and phase separation. At first, with increasing HDI/IPDI ratio, the degree of hydrogen bonding increased, which decreased the mobility of the polymer chains, resulting in an increase of the storage modulus. However, a larger HDI/IPDI ratio could cause a greater degree of phase separation. This might dramatically reduce the covalent linkages between soft segment and hard segment to restrict the segmental motion<sup>30</sup>, and predominantly affect the viscoelastic behaviour of WPUU films, leading to decreased storage modulus of the WPUU films.

As shown in **Figure 8**, the peak of  $\tan \delta$  shifted to a lower temperature, from  $-39.5\text{ }^{\circ}\text{C}$  to  $-42.6\text{ }^{\circ}\text{C}$  as the HDI/IPDI ratio increased, indicating a decrease of  $T_{gss}$ . This confirms that

**Figure 5.** AFM phase images of (a) WPUU-1 and (b) WPUU-5

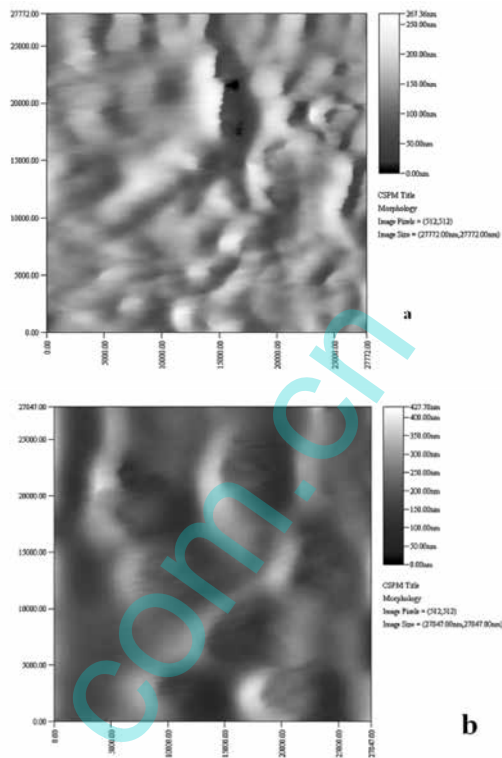
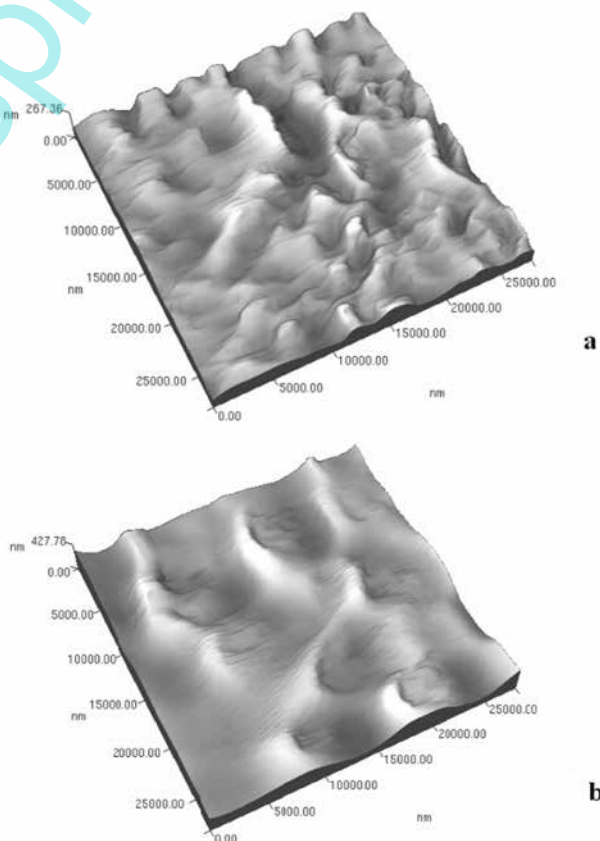


**Figure 6.** Three-dimensional AFM phase images of (a) WPUU-1 and (b) WPUU-5



the phase separation was improved, and similar results were obtained from DSC analysis. The intensity of the  $\tan \delta$  curve is lowest when HDI/IPDI ratio is 4:1. This might be attributed to the improvement of the hydrogen bonding degree and the extent of phase separation, which increases the restriction of segmental motion.

The storage modulus curve and the  $\tan \delta$  curve exhibit a shoulder from 0 °C to 50 °C. This can be contributed to the crystallization of soft segments<sup>31</sup>.

### 3.6 Mechanical Properties

The mechanical properties of WPUU depend on their microphase morphology, including the hydrogen bonding degree in the hard segments, the extent of phase separation and the segmental crystallization<sup>32</sup>. The stress-strain curves of the WPUU films are shown in **Figure 9**, and the results from these curves are listed in **Table 5**. Due to the high crystallinity of the WPUU films, all samples showed typical crystalline polymer tensile properties with yield points observed in the stress-strain curves. From the **Table 5**, it can be found that the tensile strength increased first and then decreased as HDI/IPDI ratio increased, and the WPUU-4 film exhibited a maximum tensile strength of 42.2 MPa. This might be due to the enhanced ordered hydrogen-bonding degree in the hard segments, as well as to an associated phase separation in WPUU-4, in which the hard segments act as enhanced physical crosslinking sites in the soft matrix. Although the hydrogen bonding degree of WPUU-5 is higher than that of other samples, the tensile strength of WPUU-5 decreased due to the lack of rigid aliphatic rings and the excessive phase separation degree. Thus, a low tensile strength was obtained when the HDI/IPDI ratio was above 4:1.

## 4. CONCLUSIONS

A series of aliphatic waterborne polyurethane-ureas (WPUU) was

Figure 7. Storage modulus ( $E'$ ) of WPUU films with different HDI/IPDI ratio

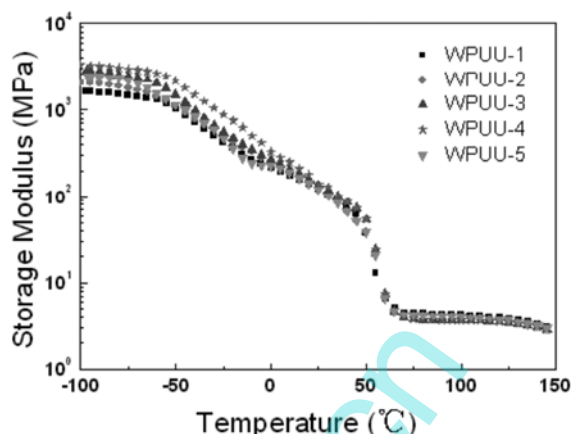


Figure 8.  $\tan \delta$  curves of WPUU films with different HDI/IPDI ratio

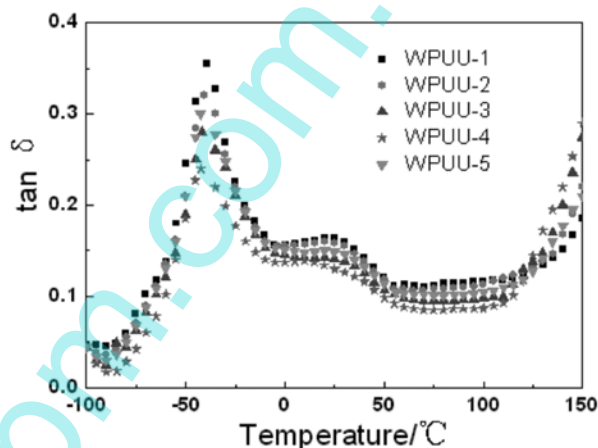


Figure 9. Stress-Strain curves of WPUU films

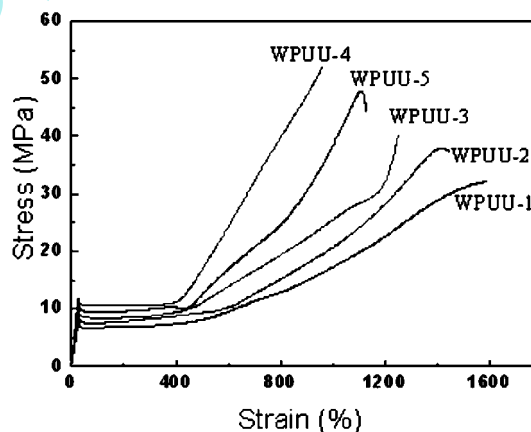


Table 5. Mechanical properties of the WPUU films with different HDI/IPDI ratio

Samples	Tensile strength (MPa)	Elongation at break (%)
WPUU-1	32.2	1589.3
WPUU-2	35.8	1401.2
WPUU-3	41.0	1113.9
WPUU-4	42.2	960.1
WPUU-5	36.1	1250.0

synthesized. The effect of HDI/IPDI ratio on the phase morphology of WPUU was studied. XRD and DSC analysis indicated that the crystallinity and the phase separation of WPUU films were improved with increasing HDI/IPDI ratio. This is attributed to the increasing degree of ordered hydrogen bonding in hard segment, resulting in enhanced thermodynamic incompatibility between soft and hard segments. AFM results verified that the extent of phase separation of WPUU was enhanced with increasing HDI/IPDI ratio. The relationship between phase morphology and dynamic mechanical properties of WPUU films was investigated by DMA. The results showed that the peak in  $\tan \delta$  shifted to a lower temperature as HDI/IPDI ratio increased, which indicated the glass transition temperature ( $T_{\text{gss}}$ ) of soft segment decreased. The storage modulus  $E'$  increased at first and then decreased, due to the effects of hydrogen bonding and phase separation in WPUU. All the WPUU films possessed excellent mechanical properties, and WPUU-4 exhibited the highest tensile strength, 42.2 MPa.

## ACKNOWLEDGMENT

We appreciate the financial support from the National Natural Science Foundation of China under grant No.21171058.

## REFERENCES

- Wang H.; Shen Y.; Fei G.; Li X.; Liang Y., Micromorphology and phase behavior of cationic polyurethane segmented copolymer modified with hydroxysilane. *Journal of Colloid and Interface Science* **324**, (2008), (1–2), 36–41.
- Cakić S.M.; Ristić I.S.; Djordjević D.M.; Stamenković J.V.; Stojiljković D.T., Effect of the chain extender and selective catalyst on thermooxidative stability of aqueous polyurethane dispersions. *Progress in Organic Coatings* **67**, (2010) (3), 274–280.
- Kultys A.; Rogulska M.; Pikus S.; Skrzypiec K., The synthesis and characterization of new thermoplastic poly(carbonate-urethane) elastomers derived from HDI and aliphatic-aromatic chain extenders. *European Polymer Journal* **45**, (9), (2009), 2629–2643.
- Bahattab M.A.; Donate-Robles, J.; García-Pacios, V.; Miguel Martín-Martínez, J., Characterization of polyurethane adhesives containing nanosilicas of different particle size. *International Journal of Adhesion and Adhesives* **31** (2), (2011) 97–103.
- Castagna A.M.; Fragiadakis D.; Lee H.; Choi T.; Runt J., The Role of Hard Segment Content on the Molecular Dynamics of Poly(tetramethylene oxide)-Based Polyurethane Copolymers. *Macromolecules* **44**, (19), (2011), 7831–7836.
- Bistričić L.; Baranović G.; Leskovic M.; Bajsić E.G., Hydrogen bonding and mechanical properties of thin films of polyether-based polyurethane-silica nanocomposites. *European Polymer Journal* **46**, (10), (2010), 1975–1987.
- Rath S.K.; Ishack A.M.; Suryavansi U.G.; Chandrasekhar L.; Patri M., Phase morphology and surface properties of moisture cured polyurethane-urea (MPCU) coatings: Effect of catalysts. *Progress in Organic Coatings* **62**, (4), (2008), 393–399.
- Park K.; Lim W.H.; Ko E.-A.; Lee H.S., Effect of molecular shape of diisocyanate units on the microscopic/macrosopic phase separation structure of polyurethanes. *Journal of Polymer Science Part B: Polymer Physics* **49**, (12), (2011), 890–897.
- Williams S.R.; Wang W.Q.; Winey K.I.; Long T.E., Synthesis and Morphology of Segmented Poly(tetramethylene oxide)-Based Polyurethanes Containing Phosphonium Salts. *Macromolecules* **41**, (23), (2008), 9072–9079.
- Luo Y.L.; Miao Y.; Xu F., Synthesis, phase behavior, and simulated in vitro degradation of novel HTPB-b-PEG polyurethane copolymers. *Macromolecular Research* **19**, (12), (2011) 1233–1241.
- Mishra, A.; Maiti, P., Morphology of Polyurethanes at Various Length Scale: The Influence of Chain Structure. *Journal of Applied Polymer Science* **120**, (6), (2011), 3546–3555.
- Sheth J.P.; Wilkes G.L.; Fornof A.R.; Long T.E.; Yilgor I. *Macromolecules* **38**, (2005), 5681
- Jelena Culin, Ivan Smit, Zorica Vekšli, et al. Phase morphology of functionalized polyester polyurethanes. Effect of functional group concentration. *Polymer International*, **55** (2006) 285–291
- Prisacariu C.; Scortanu E., Sensitivity to the Physical and Chemical Structure of Hard-Segment-Reinforced Polyurethane Elastomers with Variable Percentage of Hydrogen Bonding. *Journal of Applied Polymer Science* **122**, (6), (2011) 3544–3550.
- Rueda-Larraz L.; d'Aras B.F.; Tercjak A.; Ribes A.; Mondragon I.; Eceiza A., Synthesis and microstructure-mechanical property relationships of segmented polyurethanes based on a PCL-PTHF-PCL block copolymer as soft segment. *European Polymer Journal* **45**, (7), (2009) 2096–2109.
- Biamond G.J.E.; Brasspenning K.; Gaymans R.J., Synthesis and selected properties of polyurethanes with monodisperse hard segments based on hexane diisocyanate and three types of chain extenders. *Journal of Applied Polymer Science* **124**, (2), (2012) 1302–1315.
- Wang K.; Peng Y.; Tong R.; Wang Y.; Wu Z., The Effects of Isocyanate Index on the Properties of Aliphatic Waterborne Polyurethaneureas. *Journal of Applied Polymer Science* **118**, (2), (2010) 920–927.
- Kojio K.; Nakashima S.; Furukawa M., Microphase-separated structure and mechanical properties of norbornane diisocyanate-based polyurethanes. *Polymer* **48**, (4), (2007) 997–1004.
- Wingborg N., Increasing the tensile strength of HTPB with different isocyanates and chain extenders. *Polymer Testing* **21**, (3), (2002) 283–287.
- Lu Y.; Tighzert L.; Dole P.; Erre D., Preparation and properties of starch thermoplastics modified with waterborne polyurethane from

- renewable resources. *Polymer* **46**, (23), (2005) 9863-9870.
21. Yilgor I.; Yilgor E.; Das S.; Wilkes G.L., Time-Dependent Morphology Development in Segmented Polyetherurea Copolymers Based on Aromatic Diisocyanates. *Journal of Polymer Science Part B: Polymer Physics* **47**, (5), (2009) 471-483.
22. Krol P., Synthesis methods, chemical structures and phase structures of linear polyurethanes. Properties and applications of linear polyurethanes in polyurethane elastomers, copolymers and ionomers. *Progress in Materials Science* **52**, (6), (2007) 915-1015.
23. Tatai L.; Moore T.G.; Adhikari R.; Malherbe F.; Jayasekara R.; Griffiths I.; Gunatillake P.A., Thermoplastic biodegradable polyurethanes: The effect of chain extender structure on properties and in-vitro degradation. *Biomaterials* **28**, (36), (2007) 5407-5417.
24. Mizanur Rahman M.; Kim H.-D., Effect of polyisocyanate hardener on adhesive force of waterborne polyurethane adhesives. *Journal of Applied Polymer Science* **104**, (6), (2007) 3663-3669.
25. García-Pacios V.; Costa V.; Colera M.; Miguel Martín-Martínez J., Affect of polydispersity on the properties of waterborne polyurethane dispersions based on polycarbonate polyol. *International Journal of Adhesion & Adhesives* **30**, (6), (2010) 456-465.
26. Liow S.S.; Lipik V.T.; Widjaja L.K.; Venkatraman S.S.; Abadie M.J.M., Enhancing mechanical properties of thermoplastic polyurethane elastomers with 1,3-trimethylene carbonate, epsilon-caprolactone and L-lactide copolymers via soft segment crystallization. *Express Polymer Letters* **5**, (10), (2011) 897-910.
27. Klinedinst D.B.; Yilgör E.; Yilgör I.; Beyer F.L.; Wilkes G.L., Structure-property behavior of segmented polyurethaneurea copolymers based on an ethylene-butylene soft segment. *Polymer* **46**, (23), (2005) 10191-10201.
28. Gireesh K.B.; Jena K.K.; Allauddin S.; Radhika K.R.; Narayan R.; Raju K.V.S.N., Structure and thermo-mechanical properties study of polyurethane-urea/glycidoxypropyltrimethoxysilane hybrid coatings. *Progress in Organic Coatings* **68**, (3), (2010) 165-172.
29. Alexandru M.; Cazacu M.; Cristea M.; Nistor A.; Grigoras C.; Simionescu B.C., Poly(siloxane-urethane) crosslinked structures obtained by sol-gel technique. *Journal of Polymer Science Part A: Polymer Chemistry* **49**, (7), (2011) 1708-1718.
30. Wang K.; Peng Y.; Tong R.; Wang Y.; Wu Z., The effects of isocyanate index on the properties of aliphatic waterborne polyurethaneureas. *Journal of Applied Polymer Science* **118**, (2010), 920-927.
31. Aurilia M.; Piscitelli F.; Sorrentino L.; Lavorgna M.; Iannace S., Detailed analysis of dynamic mechanical properties of TPU nanocomposite: The role of the interfaces. *European Polymer Journal* **47**, (5), (2011), 925-936.
32. Yang C.-Z.; Grasel T.G.; Bell, J.L.; Register R.A.; Cooper S.L., Carboxylate-containing chain-extended polyurethanes. *Journal of Polymer Science Part B: Polymer Physics* **29**, (5), (1991) 581-588.